Proceedings of the 2nd Marine Energy Technology Symposium
METS2014
April 15-18, 2014, Seattle, WA

NUMERICAL OPTIMIZATION OF A PORTABLE HYDROKINETIC TURBINE

William C. Schleicher Jacob Riglin Alparslan Oztekin[1]
Department of Mechanical Engineering and Mechanics, Lehigh University
Bethlehem, Pennsylvania, USA

Robert C. Klein
e-Harvest, Inc.
Glen Gardner, New Jersey, USA

[1]Corresponding author: alo2@lehigh.edu

ABSTRACT

Hydropower has a long history as a source for clean, renewable energy. Conventional hydropower requires large civil structures and a high capital cost for construction. Hydrokinetic turbines do not require these structures and can be made to be portable systems, making them an attractive alternative to conventional hydropower. A portable hydrokinetic turbine is under development for a system that would provide soldiers with power for communication and computing devices in remote environments. A design optimization strategy is explained to optimize a turbine-diffuser system for a 2.25 m/s free-stream velocity with future plans to optimize the system at 1 m/s. The first iteration of the optimization loop is demonstrated and the results indicate an optimized design will produce 775 W. Comments on judging the results and how to proceed with the design optimization are discussed. Future plans for system design and prototype testing are provided.

INTRODUCTION

Conventional hydropower produces nearly 80 GW of energy annually in the United States, amounting to approximately half of the nation's renewable energy capacity [1]. However, conventional hydropower requires large capital investments, especially in civil structures such as dams, and can have negative consequences on the local aquatic environment. Marine and hydrokinetic (MHK) technology does not require these civil structures, thus offering an advantage over conventional hydropower. These technologies are not as mature as conventional hydropower systems in terms of design and implementation; however, in the United States, the Mississippi River alone is approximately 3,544 km (2,202 miles) in length and a significant portion of the river remains untapped for power generation. MHK technologies have the potential to capture some of this available energy [2].

Micro-hydro refers to projects that generate between 0.5 kW to 100 kW of power, which is the amount of power typically required by a single family home or a small business [3]. Small hydrokinetic systems fall within this micro-hydro category and offer portability. These characteristics are especially desirable in temporary encampment situations such as military field operations. A photovoltaic battery system called the Ground Renewable Expeditionary Energy System, or GREENS, has been developed for use by the U.S. Marine Corps to produce 300 W of continuous power to run these encampments [4]. However, when sunlight is not available, a secondary source of energy is needed to power necessary equipment. A micro-hydrokinetic system could potentially interface with this system to provide the required power.

Hydrokinetic turbines are a popular research topic, with engineers investigating multiple configurations. Batten *et al*. [5-7] used a blade element methodology (BEM) approach for horizontal axis tidal turbines. They validated their method using a scaled model in a cavitation tunnel, and concluded that their BEM model agreed with their experiments. Mukherji *et al.* [8] compared BEM with CFD for a horizontal axis hydrokinetic turbine, and determined the effect of solidity, angle of attack, and number of blades on power generation. Myer and Bahaj [9] conducted experiments on a horizontal axis turbine and concluded that the blade twist distribution, centrifugal force at the surface of the blade, lift

and drag performance, and rotor yaw angle affect the stall delay of the hydrofoil sections and thus can affect the power output from the rotor. Hwang *et al*. [10] studied a vertical axis turbine that actively controlled blade angle of attack to maximize power output and improved self-start. They showed that by individually controlling each blade's angle of attack based on the oncoming flow that there was a 25% improvement in performance compared to pure cycloidal motion for the same operating conditions.

A preliminary micro-hydrokinetic turbine blade design was previously proposed with the design goal to continuously generate 500 W of power [11]. In order to broaden the operating range of fluid speed and generate as much power as possible, the blade design must be optimized in a planned, controlled manner. A response surface methodology was chosen to optimize the design. This method provides a systematic design strategy by changing all variables at the same time. This allows for optimum conditions to be found regardless of initial values. Changing one variable at a time while holding other variables constant is a common approach to optimization, however, it is inefficient and usually unsuccessful at arriving at an optimized design.

OPTIMIZATION METHOD

The employed optimization flow chart is depicted in Figure 1. A diffuser was added to the preliminary blade design [11] because it was found to increase power production over the blade's entire designed tip-speed ratio. The first step in the design optimization scheme is to define the goals of the optimization. The design goal explored in this manuscript was to maximize power production from the turbine blades, while checking to be sure that the designed condition was structurally sound for a free-stream flow of 2.25 m/s and a rotation rate of 150 RPM. These operating conditions, however, are rare for most rivers and streams in the United States. When this optimization scheme is implemented in future design iterations, slower fluid speeds such as a 1 m/s flow will be targeted.

Once the goals of the optimization are set, the geometric parameters for the turbine-diffuser system must be selected. These design parameters are depicted in Figure 2. Figure 2A and B depicts the parameters of the turbine blades that were investigated while the variables on Figure 2C show how the diffuser was parameterized. These parameters are defined in Table 1.

The next step is to define the limits on the design space to be studied. This can be difficult to do on the first design iteration because the global minima or maxima may not actually be in that

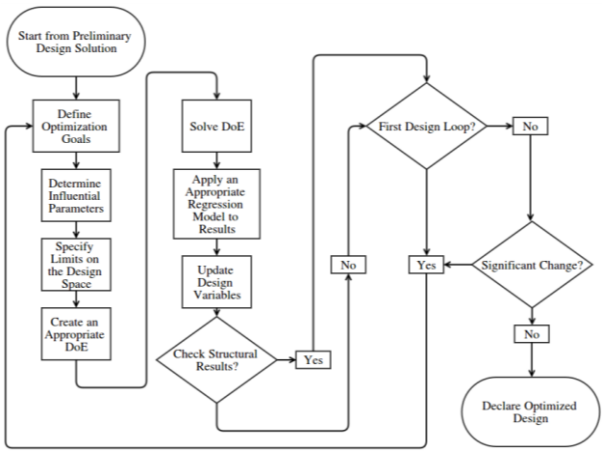

FIGURE 1. TURBINE BLADE AND DIFFUSER OPTIMIZATION FLOW CHART

TABLE 1. DESIGN VARIABLES EXPLORED

Variable	Definition
$\Delta\theta$	Blade Wrap Angle [°]
Δm	Blade Meridional Height [m]
Z_B	Number of Blades
D_{in}	Diffuser Inlet Diameter [m]
D_{out}	Diffuser Outlet Diameter [m]
L_{LE}	Blade Leading Edge Position from Inlet[%]
θ	Diffuser Angle [°]

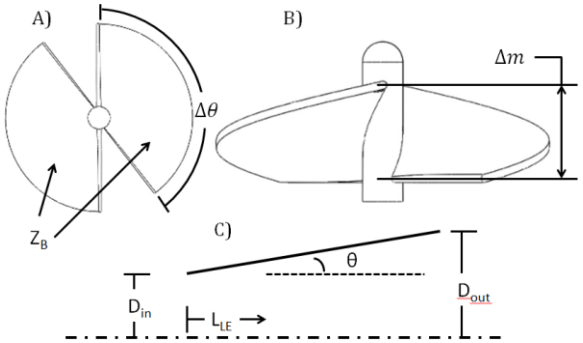

FIGURE 2. DESIGN PARAMETERS INVESTIGATED

range. Therefore, for the first design iteration it is suggested that the design space be as large as possible. If at the end of the first design iteration the design goals are met on the edge of the design space for any variable, the design space should be adjusted further in that direction in an attempt to bring the maxima or minima into the design space.

Once the design space has been limited, it is time to determine what experiments need to be run. In order to determine minima or maxima within the design space the results need to be modeled with at least a second-order regression. This requires that for each design variable m, there should be at least three levels of values for each design variable: a low, intermediate, and high

value. This gives rise to a full-factorial experiment where the number of experiments required to define the design space is given by $n = 3^m$. A problem with this design is that the number of experiments increases very rapidly with m. A central composite design of experiments offers the same functionality as a 3^m full-factorial experiment, but with less experiments needed to define the design space [12]. This, from a statistical analysis perspective, is due to the sparsity-of-effects principle, which states that the system output is usually dominated by the main design variable effects and lower-order interactions between the design variables. This methodology reduces the number of required experiments to $n = 2^m + 2m + 1$ [13]. More information on these experimental designs can be found in Box and Wilson's manuscript [14]. From these seven design variables, it was determined that 135 simulations were needed to characterize the response surface. These simulations were solved and populated the response surface.

After the results for the simulations have been obtained, an appropriate regression model must be chosen to model the data. Two regression models were investigated: a non-parametric regression [15] and a Gaussian process regression [16]. Once an appropriate regression has been selected, the optimized design must be determined from the regression model. Potential candidate points can be found either by screening through the regression model or applying a numerical scheme to find minima or maxima. Simulations are run at the potential candidate points to confirm that the regression results are correct. Once the results are verified, an optional structural analysis can take place to ensure that the new design is structurally sound.

It is then recommended that this process be repeated and the design goals reevaluated. Once the optimization process has gone through enough iterations that the investigated design parameters are not changing between iterations, the design is declared to be optimized.

RAPID CFD METHODOLOGY

While CFD simulations can generate accurate results, they can also be very time consuming. In the conventional definition of a converged solution, two conditions must be met: the maximum normalized residuals of all solved equations should decrease seven orders of magnitude and all monitored quantities should not change with subsequent iteration. These conditions make the proposed optimization scheme very time consuming due to the amount of simulations required, even when high performance computing resources are available.

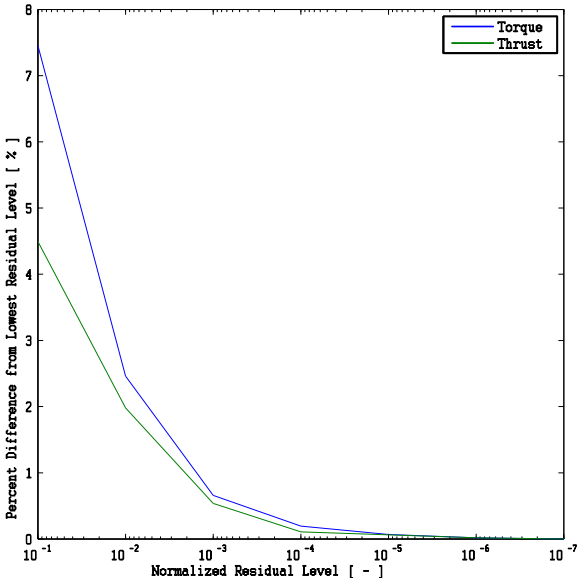

FIGURE 3. PERCENT DIFFERENCE IN CALCULATED TORQUE AND THRUST VERSUS NORMALIZED RESIDUAL RESOLUTION

In order decrease the computational time needed to run the simulations, a less stringent convergence criterion is used. CFD simulations are run until they converge well enough to get a good estimate of the optimization output quantities such as the power and thrust produced by the turbine blades.

Caution must be applied though when judging the merits of a partially converged solution. The user must bear in mind the effects of discretization and level of convergence on the sensitivity of the results. Figure 3 shows a plot of the percent difference in torque and thrust on the turbine blades versus their normalized residual level of convergence for the pressure correction equation. From this plot, it can be seen that a normalized residual level of 10^{-3} provides less than a 1% difference in the solution for torque and thrust compared to the solution at a normalized residual level of 10^{-7}. In order to allow more rapid CFD calculations during the optimization loop, a solution that has a normalized residual level of convergence of 10^{-3} in the pressure correction equation was chosen.

The same computational method, domain, and discretization method is used in this optimization study as was presented in an earlier work [11] with the several exceptions. The computations were carried out with the steady-state SIMPLE segregated solver method with multiple frames of reference instead of a transient solver. Turbulence modeling was accomplished using Menter's k-ω SST [17&18] two-equation eddy-viscosity model. This model offers improved prediction of adverse pressure gradients in the near wall region as compared to the standard k-ω and k-ε models by

incorporating Bradshaw's observation that turbulent shear stress is proportional to the turbulent kinetic energy in the wake region of the boundary layer [17]. The equations for kinematic eddy viscosity, turbulent kinetic energy, and specific dissipation rate, respectively, are shown in Equation (1).

$$\nu_T = \frac{\alpha_1 k}{\max(\alpha_1 \omega, SF_2)}$$

$$\frac{\partial k}{\partial t} + U_j \frac{\partial k}{\partial x_j} = \tau_{ij} \frac{\partial U_i}{\partial x_j} - \beta^* k\omega + \frac{\partial}{\partial x_j}\left[(\nu + \sigma_k \nu_T)\frac{\partial k}{\partial x_j}\right]$$

$$\frac{\partial \omega}{\partial t} + U_j \frac{\partial \omega}{\partial x_j} = \alpha S^2 - \beta \omega^2 + \frac{\partial}{\partial x_j}\left[(\nu + \sigma_\omega \nu_T)\frac{\partial \omega}{\partial x_j}\right] + 2(1 - F_1)\sigma_{\omega 2}\frac{1}{\omega}\frac{\partial k}{\partial x_i}\frac{\partial \omega}{\partial x_i} \quad (1)$$

Here, ν_T is the turbulent viscosity, ν is the kinematic viscosity, k is the turbulent kinetic energy, ω is the specific dissipation rate, $\alpha_1$is a closure coefficient, U is the velocity, and S is the mean rate-of-strain tensor. For the sake of brevity, the blending functions F_1 and F_2 are not shown but the implemented model uses the original implementation of the k-ω SST turbulence model.

A rotating reference frame was used in the vicinity of the turbine which transformed flow from an unsteady inertial frame to a steady non-inertial frame with the inclusion of the centrifugal and Coriolis forces into the transport equations as shown in Equation (2).

$$\frac{\partial U_{r,i}}{\partial x_i} = 0$$

$$\frac{\partial U_{r,i}}{\partial t} + U_{r,j}\frac{\partial U_{r,i}}{\partial x_j} = -\frac{1}{\rho}\frac{\partial p}{\partial x_j} - 2\epsilon_{iql}\omega_q U_{r,l} - \epsilon_{iql}\epsilon_{lst}\omega_q\omega_s x_t + \nu\frac{\partial^2 U_{r,i}}{\partial x_q \partial x_q} \quad (2)$$

Here, U_r is the velocity relative to the rotating frame of reference. The position is represented by x and time by t. Static pressure is depicted as p, density by ρ, angular rotation rate of the frame of reference by ω, ε is the permutation symbol and the subscripts i, j, l, q, s, and t are index placeholders.

TABLE 2. DESIGN SPACE INVESTIGATED

Variable	Low Value	High Value
$\Delta\theta$	35°	145°
Δm	1.5 in	5.5 in
Z_B	2	6
D_{in}	21 in	23.1 in
D_{out}	26.25 in	36.75 in
L_{LE}	25%	75%
θ	5°	20°

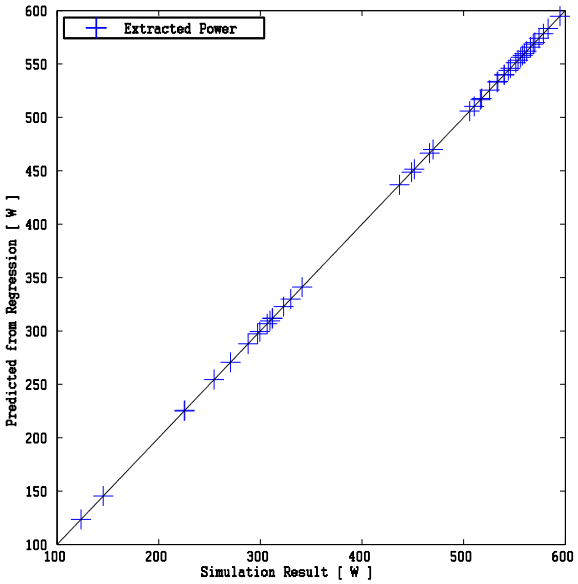

FIGURE 4. REGRESSION PREDICTED OUTPUT POWER VERSUS SIMULATION PREDICTED OUTPUT POWER

RESULTS FROM ONE OPTIMIZATION LOOP

One loop of this optimization methodology has been tested with the variables depicted in Figure 2 and Table 1 for a free stream flow condition of 2.25 m/s with a constant rotation rate of 150 RPM. In order to broaden potential deployment sites, future designs will be explored at much lower fluid speeds.

The design space for this preliminary design iteration is depicted in Table 2. The design space was chosen based on portability concerns and previous experimentation with the design variables. A total of 135 simulations were conducted over a two week period on a state-of-the-art desktop PC. Simulations were run sequentially with a run time of 2.5 hours per simulation.

Regression models described in the previous section were applied to the simulation results. Only the results from the non-parametric regression analysis are presented here, since the Gaussian process regression model predicted similar results. Figure 4 shows a Goodness of Fit plot of the non-parametric regression's prediction of power versus the simulation result of predicted

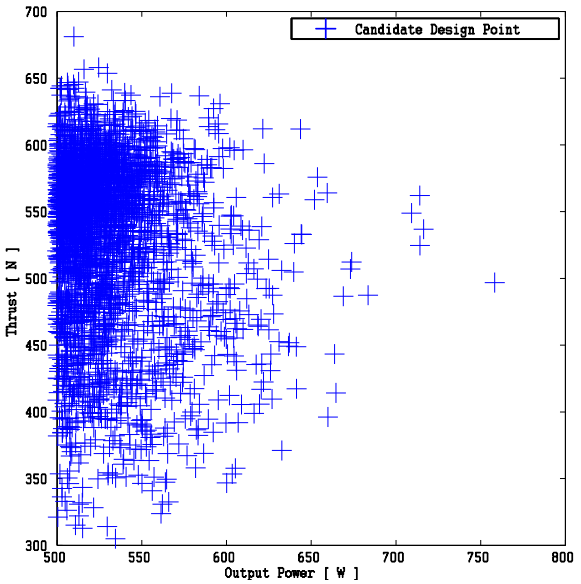

FIGURE 5. CANIDATE DESIGN POINT TRADEOFFS BETWEEN OUTPUT POWER AND THRUST

power. The regression model fit very well with the simulation results, yielding a coefficient of determination of one and a root mean square error of 2.8379 x 10^{-6}.

Both a screening and max-min algorithm method were applied to the regression model in order to determine the combination of design variables that would maximize the output power of the turbine. Once candidate points that satisfied the design goal were determined, simulations were conducted to verify the regression model's predictions. Table 3 displays three candidate points that maximized power output from the regression model. It also shows what the regression model predicted for power generation, the simulation verified the power, and the percent difference between the values. The results demonstrate that the regression model and rapid CFD simulations agreed well, predicting the power generation within 6% of each other. However, these results should not yet be accepted as the true predicted result for power generation because of the assumptions made regarding the domain discretization and the acceptable normalized residual error. A more spatially resolved CFD analysis of the candidate points is required. Nevertheless, these initial results help to narrow-in on candidate points for further investigation.

Once candidate points are verified using rapid CFD analysis, a structural analysis may be performed to ensure that the points are structurally sound. This analysis is usually one-way coupled, where the results from the CFD analysis are used as boundary conditions for the structural analysis. The deflections calculated in the structural analysis do not affect the flow

TABLE 3. CANDIDATE DESIGN POINTS AND THEIR PREDICTED POWER GENERATION FROM THE REGRESSION AND SIMULATION ANALYSIS

	Candidate A	Candidate B	Candidate C
$\Delta\theta$	88.8260°	87.4607°	85.4050°
Δm	5.2637 in	5.2786 in	5.1819 in
Z_B	6	6	6
D_{in}	22.0585 in	22.0621 in	22.0553 in
D_{out}	31.6590 in	31.7532 in	31.7901 in
L_{LE}	48.6%	48.3%	48.5%
θ	12.9228°	13.2441°	13.4557°
$P_{Reg.}$	759 W	757 W	754 W
$P_{Sim.}$	773 W	784 W	799 W
Diff.	1.81%	3.36%	5.64%

simulations in a one-way coupled analysis. A two-way coupled analysis would be required for this type of interaction between fluid and structural analysis. Two-way coupled simulations require transient analysis and significantly increase computational time, therefore it is recommended to use a one-way analysis for this optimization scheme. With a one-way coupled analysis, the pressure information from the CFD analysis is interpolated onto the structural mesh and used to load the blades. The blades are allowed to rotate freely, but are fixed from moving axially. Inertial effects are also considered in the analysis. The results from these simulations give insight into the stresses and deflections present in the mechanical design of the blades. Preliminary structural results show that for aluminum blades, the candidate points are an order of magnitude away from yield, and the maximum deflection is on the order of a tenth of a millimeter.

To continue with the optimization method described above, the designer should go through another iteration starting at defining the goals for this loop. The designer should also reevaluate the design variables and remove any variables deemed insignificant or add new variables. Based on the results from the first iteration, the limits of the design space should be narrowed to pinpoint an optimized design. A variety of flow conditions should be tested to ensure that the system performs well over the expected range of operating conditions. Once the designer is confident that the design variables are not changing significantly between iterations, the design may be deemed optimized.

CONCLUSIONS AND FUTURE WORK

A methodology has been presented to optimize a turbine blade and diffuser system. The central composite design of experiments methodology was used to determine the simulations required to explore the design

variables in question. The non-parametric regression was employed to model the response surface of the design variables from the rapid CFD results. The regression model fit very well with the simulation data.

The computational domain was coarsely discretized and solutions for the rapid CFD simulations were only required to drop three orders of magnitude in the normalized residuals before calling a solution converged. These previsions allowed a general idea of basic performance characteristics to be obtained while keeping computational time to a minimum in order to complete the number of simulations required to generate a response surface.

The predicted maximized power generation from the non-parametric regression model matched the verified rapid CFD results within 6%. The results from the first iteration of design optimization indicate that maximum power generation for the system at a flow rate of 2.25 m/s and turbine rotation rate of 150 RPM is around 775 W. Further design iterations, design iterations at more tip speed ratios, and a more refined CFD study are required before deeming the turbine-diffuser system optimized.

Future design iterations will optimize the turbine-diffuser system for a best efficiency point at a 1 m/s free-stream velocity. The full system design including generator, mechanical design, nacelle, and mooring will soon be finalized. Prototype testing is expected to begin late 2014 at the David Taylor Model Basin in Bethesda, Maryland.

ACKNOWLEDGEMENTS

The authors would like to gratefully acknowledge funding from the Office of Naval Research for this work under Award N00014-12-M-0050. The authors would also like to thank Suzanne DiNello for her help in preparing this manuscript.

REFERENCES

[1] J. J. Conti, J. A. Bearmon, S. A. Napolitano, A. M. Schaal and J. T. Turnure, "Annual Energy Outlook 2013 with Projections to 2040," U.S. Energy Information Administration, Washington, DC, 2013.

[2] A. C. Benke and C. E. Cushing, Rivers of North America, Burlington: Academic Press, 2005.

[3] D. Jenkins, Renewable Energy Systems: The Earthscan Expert Guide to Renewable Energy Technologies for Home and Business, Florence: Taylor and Francis, 2013.

[4] U.S. Marine Corps, "Guide to Employing Renewable Energy and Energy Efficient Technologies," Marine Corps Warfighting Laboratory, Quantico, 2012.

[5] W. M. J. Batten, A. S. Bahaj, A. F. Molland and J. R. Chaplin, "Experimentally validated numerical method for the hydrodynamic design of horizontal axis tidal turbines," *Ocean Engineering,* vol. 34, pp. 1013-1020, 2007.

[6] W. M. Batten, A. S. Bahaj, A. F. Molland and J. R. Chaplin, "Hydrodynamics of marine current turbines," *Renewable Energy,* vol. 31, pp. 249-256, 2006.

[7] W. M. Batten, A. S. Bahaj, A. Molland and J. R. Chaplin, "The prediction of the hydrodynamic performance of marine current turbines," *Renewable Energy,* vol. 33, pp. 1085-1096, 2008.

[8] S. S. Mukherji, N. Kolekar, A. Banerjee and R. Mishra, "Numerical investigation and evaluation of optimum hydrodynamic performance of a horizontal axis hydrokinetic turbine," *Journal of Renewable and Sustainable Energy,* vol. 3, pp. 1-18, 2011.

[9] L. Myers and A. S. Bahaj, "Power output performance characteristics of a horizontal axis marine current turbine," *Renewable Energy,* vol. 31, pp. 197-208, 2006.

[10] I. S. Hwang, Y. H. Lee and S. J. Kim, "Optimization of cycloidal water turbine and the performance improvement by individual blade control," *Applied Energy,* vol. 86, pp. 1532-1540, 2009.

[11] W. C. Schleicher, J. D. Riglin, Z. A. Kraybill, A. Oztekin and R. C. Klein, Jr., "Design and Simulation of a Micro Hydrokinetic Turbine," in *Proceedings of the 1st Marine Energy Technology Symposium*, Washington, D.C., 2013.

[12] R. H. Myers, Responce Surface Methodology, Boston: Allyn and Bacon, Inc., 1971.

[13] J. Ledolter and R. V. Hogg, Applied Statistics for Engineers and Physical Scientists, Upper Saddle River: Pearson Prentice Hall, 2010.

[14] G. E. P. Box and K. B. Wilson, "On the Experimental Attainment of Optimum Conditions," *Journal of the Royal Statistical Society. Series B (Methodological),* vol. 13, no. 1, pp. 1-45, 1951.

[15] A. W. Bowman and A. Azzalini, Applied smoothing techniques for data analysis : the kernel approach with S-Plus illustrations, New York: Oxford University Press, 1997.

[16] W. H. Press, S. A. Teukolsky, W. T. Vetterling and B. P. Flannery, Numerical Recipes: The Art of Scientific Computing, New York:

Cambridge University Press, 2007.

[17] F. R. Menter, "Two-Equation Eddy-Viscosity Turbulence Models for Engineering Applications," *AIAA Journal,* vol. 32, no. 8, pp. 1598-1605, 1994.

[18] F. R. Menter, "Zonal Two Equation k-ω Turbulence Models for Aerodynamic Flows," *AIAA Paper 93-2906.*